Chapter 2

Effect of Dopants on the Properties of Zirconia-Supported Iron Catalysts for Ethylbenzene Dehydrogenation with Carbon Dioxide

Maria do Carmo Rangel, Sirlene B. Lima,
Sarah Maria Santana Borges and
Ivoneide Santana Sobral

Additional information is available at the end of the chapter

http://dx.doi.org/10.5772/64186

Abstract

Due to the harmful effects of carbon dioxide to the environment, a lot of work has been carried out aiming to find new applications, which can decrease the emissions or to capture and use it. An attractive application for carbon dioxide is the synthesis of chemicals, especially for producing styrene by ethylbenzene dehydrogenation, in which it increases the catalyst activity and selectivity. In order to find efficient catalysts for the reaction, the effect of cerium, chromium, aluminum, and lanthanum on the properties of zirconia-supported iron oxides was studied in this work. The modified supports were prepared by precipitation and impregnated with iron nitrate. The obtained catalysts were characterized by thermogravimetry, Fourier transform infrared spectroscopy, X-ray diffraction, specific surface area measurement, and temperature-programmed reduction. The catalysts showed different textural and catalytic properties, which were associated to the different phases in the solids, such as monoclinic or tetragonal zirconia, hematite, maghemite, cubic ceria, monoclinic or hexagonal lantana, and rhombohedral chromia, the active phases in ethylbenzene dehydrogenation. The most promising dopant was cerium, which produces the most active catalyst at the lowest temperature, probably due to its ability of providing lattice oxygen, which activates carbon dioxide and increases the reaction rate.

Keywords: carbon dioxide, styrene, ethylbenzene, dehydrogenation, zirconia, iron oxide

1. Introduction

3 Although greenhouse gas emissions are reaching alarming rates, 80% of the world's energy consumption still comes from fossil fuels, which have been pointed out as the largest source of carbon dioxide emissions [1]. Over the past decade, the global emissions of carbon dioxide from fossil fuels have increased by 2.7% each year and currently are 60% above the levels registered in 1990, which is considered the reference year for the Kyoto Protocol [2]. On the other hand, it is expected that carbon dioxide emissions should reduce by at least 50% to limit the rise of the global average temperature to 2°C by 2050 [3]. Nowadays, the major environmental concerns worldwide, global warming and the acidification of the oceans, are mainly ascribed to the increase of carbon dioxide concentration [4, 5]. Therefore, several alternatives have been proposed to decrease the carbon dioxide concentration and then to mitigate the environment changes. They include demand-side conservation, supply-side efficiency improvement, increasing reliance on nuclear and renewable energy, and carbon capture and storage (CCS) systems [6]. Among them, CCS is considered the most practical approach for long-term carbon dioxide emission reductions, since fossil fuels will continue to be the major source of energy in the next future. However, there are still some technical and economic barriers to be overcome before it can be used on a large scale. One of the main obstacles is the required large capital investment, besides technical difficulties, such as carbon dioxide leakage rates and limited geological storage capacity. Other drawbacks include the costs of transportation and injection when carbon dioxide is only available offshore, such as in United Kingdom, Norway, Singapore, Brazil, and India [7, 8]. Therefore, a more suitable alternative is to capture and use carbon dioxide (carbon capture and utilization [CCU]), changing the waste carbon monoxide emissions into valuable products such as chemicals and fuels, while contributing to climate change mitigation [9].

Captured carbon dioxide can be used as a commercial product, both directly or after conversion. In food and drink industries, for instance, carbon dioxide is often used as a carbonating agent, preservative, packaging gas, and for extracting flavors, as well as in the decaffeination process. In the pharmaceutical industry, it is used as a respiratory stimulant or for the synthesis of drugs. However, these applications are restricted to high-purity carbon dioxide, as that obtained in ammonia plants [9, 10]. Moreover, pressurized carbon dioxide has been investigated for wastewater treatment and water disinfection [11]. Other direct applications of carbon dioxide include enhanced oil recovery and coal-bed methane recovery, where crude oil is extracted from an oil field or natural gas from unminable coal deposits [9].

In the production of chemicals and fuels, carbon dioxide has attracted increasing attention over several decades, for the synthesis of various fine and bulk chemicals. It has already been used in the industrial production of urea, cyclic carbonates, salicylic acid, and methanol [12]. It is expected that carbon dioxide can produce feedstock for chemical, pharmaceutical, and polymer industries by carboxylation reactions to obtain organic compounds, such as carbonates, acrylates, and polymers, or by reduction reactions, where the C=O bonds are broken to produce chemicals such as methane, methanol, syngas, urea, and formic acid [9, 13]. Carbon dioxide can have several other applications, both as carbon or oxygen sources, for the synthesis

http://dx.doi.org/10.5772/64186

of chemicals by several processes, as solvent and/or as reactants. It has potential applications in supercritical conditions, in direct carboxylation reactions, in the conversion of natural gas to liquid (GTL technology), and in methanol synthesis [14]. Carbon dioxide can also act as an oxidant in the dehydrogenation of ethane [15], propane [16], isobutene [17], and ethylbenzene [18–20], as well as in methane dry reforming [21] and oxidative coupling of methane [22]. It is expected that the 115 million metric tons of carbon dioxide, currently consumed every year as feedstock in a variety of synthetic processes, can be triplicated by the use of new technologies [19]. In addition, carbon dioxide can overcome several drawbacks of the processes, especially in the case of dehydrogenation reactions.

In industrial processes, the dehydrogenation of hydrocarbons is often carried out at high temperatures to increase the conversion because of its reversibility and limitation by thermodynamic equilibrium. Besides being an energy-consuming process, the high temperatures cause the hydrocarbons cracking, decreasing the selectivity. On the other hand, by the oxidation of the produced hydrogen or by using an oxidant in the presence of a catalyst, these difficulties can be overcome, since the oxidative dehydrogenation is exothermic and can be performed at low temperatures, making negligible the formation of cracking products. Therefore, the use of an oxidant increases the catalyst selectivity and decreases the undesirable products, besides other advantages. Among the oxidizing agents, carbon dioxide has proven to be the most promising one for dehydrogenation reactions [23]. In the ethylbenzene dehydrogenation, for instance, the use of carbon dioxide can provide a route, which represents an elegant and promising alternative to the conventional process of styrene production.

Currently, the ethylbenzene dehydrogenation in the presence of overheated steam [Eq. (1)] is the main commercial route to produce styrene, one of the most used intermediate for organic synthesis. It is the main building block for several polymers, such as polystyrene, styrene-butadiene rubber, styrene-acrylonitrile, acrylonitrile-butadiene-styrene, and other high-value products. The ethylbenzene dehydrogenation supplies 90% of the global production of styrene, which was around 30×10^6 t in 2010 [24].

$$C_6H_5CH_2CH_{3(g)} + H_2O_{(g)} \longrightarrow C_6H_5CH=CH_{2(g)} + H_{2(g)} \quad (1)$$

In spite of this fact, the commercial process still has several drawbacks, such as the high consumption of energy, the reaction endothermicity (ΔH = 124.85 kJ/mol), the equilibrium limitation of reaction, and the catalyst deactivation [25]. On the other hand, the replacement of steam by carbon dioxide leads to a consumption of $1.5–1.9 \times 10^8$ cal, instead of 1.5×10^9 cal/mol of styrene produced. In this case, hydrogen is continuously removed as steam by the reverse water gas shift reaction, and the equilibrium is shifted to the formation of dehydrogenation products [Eq. (2)]. In addition, carbon dioxide removes the coke deposits formed during the reaction [26].

$$C_6H_5CH_2CH_{3(g)} + CO_{2(g)} \longrightarrow C_6H_5CH=CH_{2(g)} + CO_{(g)} + H_2O_{(g)} \quad (2)$$

The use of carbon dioxide includes other advantages such as being an inexpensive, nontoxic, and renewable feedstock, which provides a positive impact on the global carbon balance. In addition, it can accelerate the reaction rate, improve styrene selectivity, decrease the thermodynamic limitations, suppress the total oxidation, increase the catalyst life, and avoid hotspots [27]. Therefore, the ethylbenzene dehydrogenation with carbon dioxide has been studied over several different catalysts, including iron oxide, vanadium oxide, antimony oxide, chromium oxide, cerium oxide, zirconium oxide, lanthanum oxide, perovskites, and the oxide catalysts promoted with alkali metals supported on several oxides [16, 19, 20, 24, 26–33]. In addition, several works have shown that carbon-based catalysts are active and selective to produce styrene through ethylbenzene dehydrogenation with carbon dioxide. Activated carbons [34, 35], carbon nanofibers [36], onion-like carbons [37], diamonds and nanodiamonds [37, 38], graphites [39], and multiwalled carbon nanotubes (MWCNTs) [40], among others, have been evaluated in ethylbenzene dehydrogenation.

These studies have shown that the effect of carbon dioxide on the activity, selectivity, and stability of the catalysts for ethylbenzene dehydrogenation depends on the kind of the catalyst, as well as on the reaction conditions. For zirconia-based catalysts, the positive effect of carbon dioxide was found to be highly dependent on the crystalline phase at 550°C. It was noted that the tetragonal phase showed high activity and selectivity to styrene, a fact that was related to differences in specific surface area of the solids and their affinity with carbon dioxide associated with the surface basic sites [41, 42]. In a previous work [19], we have found that zirconia was the most active and selective catalyst to produce styrene through ethylbenzene dehydrogenation with carbon dioxide, as compared to metal oxides such as lantana (La_2O_3), magnesia (MgO), niobia (Nb_2O_5), and titania (TiO_2). This finding was related to the highest intrinsic activity of zirconia.

In spite of the numerous studies on the catalyst properties for the dehydrogenation of ethylbenzene in the presence of carbon dioxide, no satisfactory catalyst was found yet, requiring new developments. In the present work, the effect of cerium, chromium, aluminum, and lanthanum on the properties of zirconia-supported iron oxides was studied aiming to find efficient catalysts for the reaction.

2. Experimental

2.1. Catalysts preparation

The precursor of zirconium oxide was obtained by hydrolysis of zirconium oxychloride (1 mol/l) with an ammonium hydroxide solution (30% w/v). The obtained gel was rinsed with an ammonium hydroxide solution (1% w/v) eight times up not to detect chloride ions by Mohr's method anymore. The gel was then dried in an oven at 120°C, for 12 h. The solid was calcined at 600°C, for 4 h, under airflow (50 ml/min).

The metal-doped zirconia samples were prepared by the same method, using solutions of zirconium oxychloride and of metal nitrates (Zr/*M* = 10), where *M* = Ce (FCEZ sample), Cr

http://dx.doi.org/10.5772/64186

(FCRZ sample), Al (FALZ sample and La (FLAZ sample). Cerium, chromium, aluminum, and lanthanum oxides were also prepared following the same procedure, using aluminum nitrate, cerium nitrate, lanthanum nitrate, and chromium nitrate, respectively, to be used as references.

The modified zirconium oxides were subsequently impregnated with an iron nitrate solution (0.17 mol/l), at room temperature, to obtain the catalysts.

2.2. Catalysts characterization

After iron impregnation, the samples (catalyst precursors) were analyzed by thermogravimetry (TG) and Fourier transform infrared spectroscopy (FTIR).

After calcination, the catalysts were characterized by Fourier transform infrared spectroscopy, X-ray diffraction (XRD), specific surface area measurement, and temperature-programmed reduction.

The experiments of thermogravimetry (TG) were performed on a Mettler Toledo TGA/SDTA 851 equipment. The sample (0.02 g) was placed in a platinum crucible and heated (10°C/min) from room temperature to 1000°C, under airflow (50 ml/min).

The presence of nitrate species in the samples was detected by FTIR, using a Perkin Elmer, Model—Spectrum One, equipment, in the range of 400–4000 cm^{-1}. The samples were prepared as potassium bromide discs, in a 1:10 proportion.

The experiments of X-ray diffraction (XRD) were carried out in a Shimadzu model XD3A apparatus, using CuKα radiation generated at 30 kV and 20 mA and nickel filter.

The specific surface areas were measured in a Micromeritics ASAP 2020, using the sample (0.2 g) previously heated at 300°C, under nitrogen flow.

The curves of temperature-programmed reduction were obtained on a Micromeritics model TPR/TPD 2900 equipment, utilizing 0.3 g of the sample, and heating the solid with a rate of 10°C/min, under flow of a mixture of 5% hydrogen in nitrogen up to 1000°C.

2.3. Catalysts evaluation in ethylbenzene dehydrogenation with carbon dioxide

The catalysts were evaluated in ethylbenzene dehydrogenation in the presence of carbon dioxide in a fixed bed reactor, using 0.3 g of catalyst, at several temperatures (530, 550, 570, 590, 610, and 630°C) under atmospheric pressure. A carbon dioxide to ethylbenzene molar ratio of 10 was used for all experiments.

The reaction products were analyzed by online gas chromatography, using a Varian Star 3600 Cx equipment with a flame ionization detector. A commercial catalyst for the ethylbenzene dehydrogenation with steam, based on iron and chromium oxides, was also evaluated in the same conditions, for comparison.

3. Results and discussion

3.1. Thermogravimetry

The TG curves for the catalyst precursors (before calcination) are displayed in **Figure 1**. For all cases, there was a weight loss in two stages: the first at around 200°C, related to loss of volatiles adsorbed on the solids; the second stage at higher temperatures, in the range of 200–450°C, can be assigned to the decomposition of iron hydroxide to produce hematite and/or maghemite [43, 44]. It can be noted that the kind of the support affected hematite formation, probably due to different interactions of the iron oxide precursor with the support. The process was easier over lanthanum-doped zirconia (225°C), followed by cerium-doped zirconia (250°C). On the other hand, for aluminum-doped zirconia (292°C) and for chromium-doped zirconia (300°C), the process was delayed, suggesting that iron hydroxide was more strongly bonded to these supports.

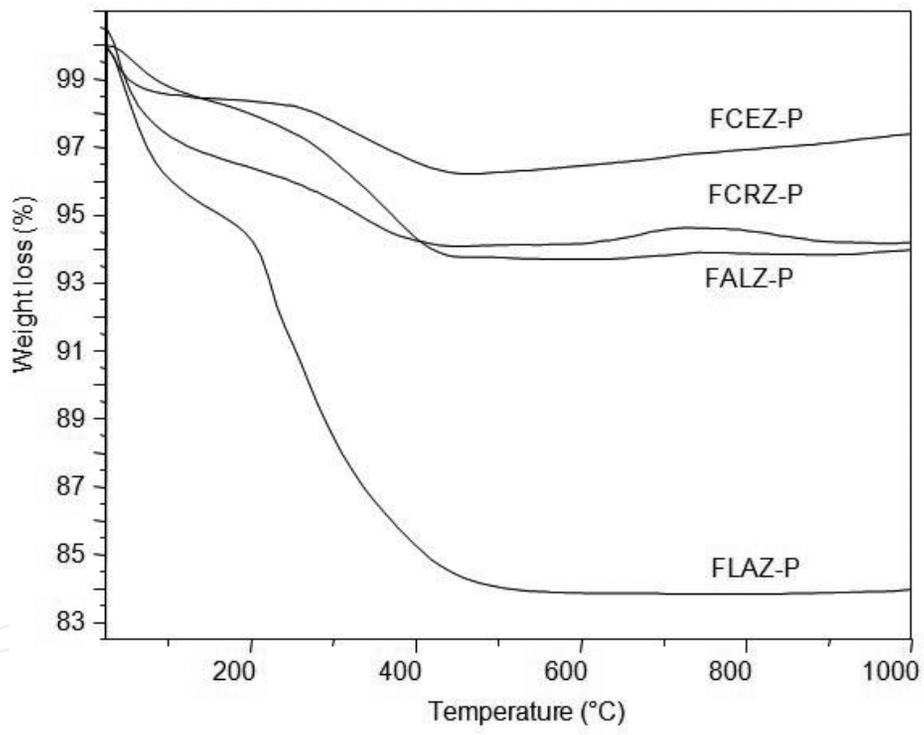

Figure 1. TG curves for the catalyst precursors. F, iron; CE, cerium; CR, chromium; AL, aluminum; LA, lanthanum; Z, zirconia.

3.2. Fourier transform infrared spectroscopy

The FTIR spectra for the precursors (**Figure 2a**) show two bands at 3400 and 1600 cm^{-1}, assigned to the bending vibrations of OH groups in iron hydroxides and in adsorbed water [45]. The absorption at 1384 cm^{-1} is related to the nitrate species [46], from iron nitrate. In the low-frequency region, a broad band was observed, in the range of 800–400 cm^{-1}, attributed to the

http://dx.doi.org/10.5772/64186

Fe–O bond [45]. For the catalysts (**Figure 2b**), it can noted that the band at 1384 cm^{-1} decreased for the samples, except for chromium-doped catalyst, indicating that the calcination was effective for the removal of nitrate species.

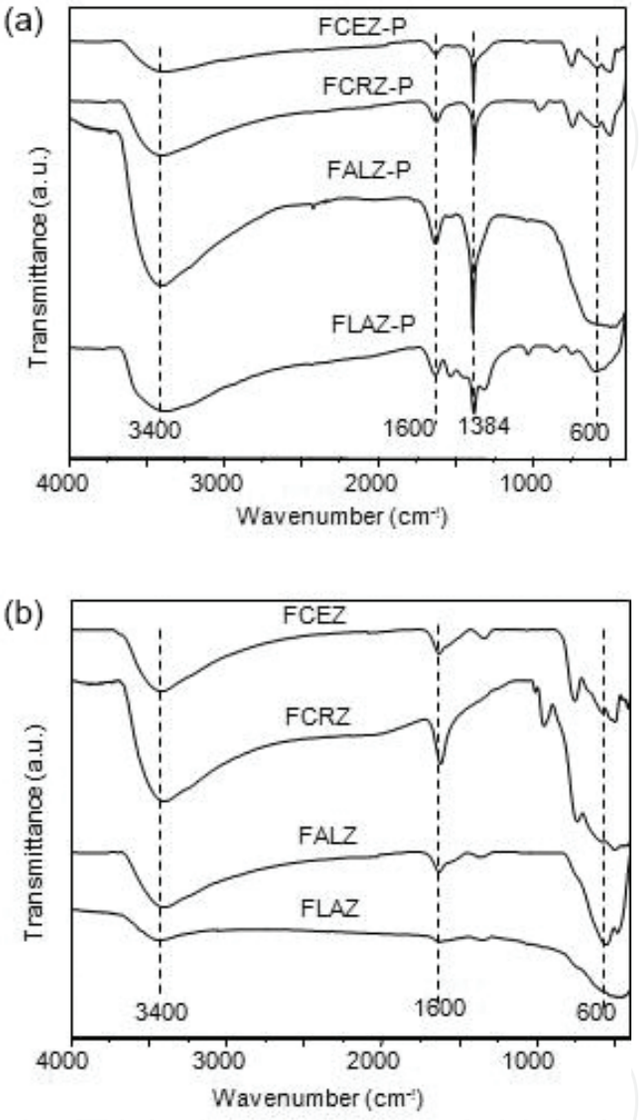

Figure 2. FTIR spectra for the precursors (P) and for the catalysts. F, iron; CE, cerium; CR, chromium; AL, aluminum; LA, lanthanum; Z, zirconia.

3.3. X-ray diffraction

From the X-ray diffractograms of the solids (**Figure 3**), different phases were found for all samples, related to the different oxides. However, for most cases, it was not possible to assure the presence of isolated phases of iron, zirconium, and of the dopants. Therefore, hematite, α-Fe_2O_3 (JCPDS 871166), maghemite, γ-Fe_2O_3 (JCPDS 251402), or zirconium oxide, ZrO_2 (monoclinic, JCPDS 830944 and tetragonal, JCPDS 881007), as well as lanthanum oxide, La_2O_3

(monoclinic, JCPDS 220641 or hexagonal, JCPDS 401279), aluminum oxide, Al_2O_3 (orthorhombic, JCPDS 880107), or chromium oxide, Cr_2O_3 (rhombohedral, JCPDS 841616), cannot be detected, because of the coincidence of the diffraction peaks of these phases. Only maghemite and the cubic phase of ceria, CeO_2 (JCPDS 780694), were detected as isolated phases for the chromium and cerium-doped samples, respectively.

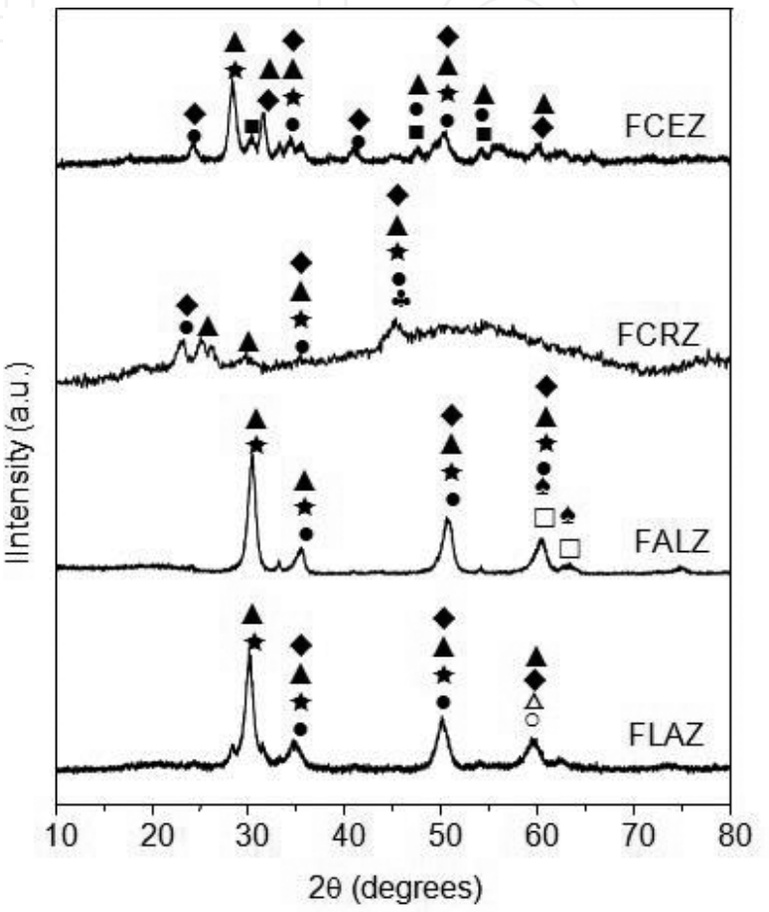

Figure 3. X-ray diffractograms for the catalysts. F, iron; CE, cerium; CR, chromium; AL, aluminum; LA, lanthanum; Z, zirconia. ♦: hematite (α-Fe_2O_3), ematite (ray dγ-Fe_2O_3, ★: tetragonal zirconia (ZrO_2), ●, monoclinic zirconia (ZrO_2), ■, cubic ceria (CeO_2), ♣: rhombohedral chromia (Cr_2O_3), Δ:hexagonal lantana (La_2O_3), ○, monoclinic lantana (La_2O_3), □: orthorhombic alumina (Al_2O_3), ♠: monoclinic alumina (Al_2O_3).

3.4. Specific surface areas

Table 1 shows the specific surface areas of the catalysts, as well as of pure and doped supports. It can be noted that pure oxides showed different values, which are typical of the nature of each oxide. Zirconia showed the highest values, while chromium showed the lowest one. In addition, the dopants changed the specific surface area of zirconia (73 m^2/g), depending on the kind of dopant. These different behaviors are related to the size of the ions, the possibility of the ion to enter into zirconia lattice, and the formation of mixed compounds. According to previous studies [47–49], it would be expected that these dopants would in-

http://dx.doi.org/10.5772/64186

crease the specific surface areas of zirconia, because of the differences in ionic radius of cerium (0.97 Å), chromium (0.615 Å), aluminum (0.54 Å), and lanthanum (1.16 Å), as compared to zirconium (0.84 Å). These differences often cause stresses in zirconia lattice, favoring the production of smaller particles, since they decrease the stress to surface ratio. However, only for the aluminum-doped zirconia the specific surface area increased, suggesting that most of the dopants did not enter into the lattice but rather remain as a segregated phase, as detected for cerium-doped zirconia.

The impregnation of iron on the supports also changes the specific surface areas, as shown in **Table 1**. For the chromium-doped and lanthanum-doped samples, the addition of iron caused an increase in specific surface area, suggesting a contribution of the iron oxides to these values. On the other hand, the other samples showed a decrease in the specific surface area, indicating that they went on sintering during the calcination step, after iron impregnation. The chromium-based catalyst showed the highest value, while the cerium-based catalyst showed the lowest one.

Samples	Sg (m^2/g)
Z	73
CE	38
CR	1.7
AL	23
LA	17
CEZ	74
CRZ	17
ALZ	98
LAZ	19
FCEZ	58
FCRZ	127
FALZ	85
FLAZ	95

Z, zirconia; CE, cerium or ceria; CR, chromium or chromia; AL, aluminum or alumina; LA, lanthanum or lanthana; F, iron oxide.

Table 1. Specific surface areas (*Sg*) of pure oxides, doped zirconia, and of iron oxide supported on doped zirconia.

3.5. Temperature-programmed reduction

The catalysts showed different reduction profiles, as displayed in **Figure 4**. The cerium-doped catalyst showed a peak beginning at 192°C and others in the range from 398 to 931°C. The first peak can be assigned to the reduction of Fe^{+3} to Fe^{+2} species, while the latter is due to the reduction of Fe^{+2} to Fe^{0} species [50], as well as to the reduction processes related to the support

[32, 33]. On the other hand, the chromium-doped zirconia sample showed a reduction peak beginning at 182°C, with a shoulder at around 274°C, as well as another peak in the range 501–929°C. The first peak can be associated to the reduction of Cr^{+6} to Cr^{+3} [16] species and of Fe^{+3} to Fe^{+2} species, while the latter one is due to the reduction of Fe^{+2} to species Fe^{0} [50]. The lanthanum-doped sample showed a peak beginning at 225°C and other ones at 327, 393, and 500°C, attributed to the reduction of Fe^{+3} species in different interactions with the support. A broad peak in the range of 600–781°C is related to the reduction of Fe^{+2} to Fe^{0} species and to the processes related to the support. For the aluminum-doped sample, two reduction peaks beginning at 200 and 332°C were noted associated to the reduction of Fe^{+3} to Fe^{+2} species in different interactions with the support. A broad peak in the range of 406–704°C can be assigned to the reduction of Fe^{+2} to Fe^{0} species. The easiness of the reduction decreased with the dopants in the order: Cr > Ce > Al > La.

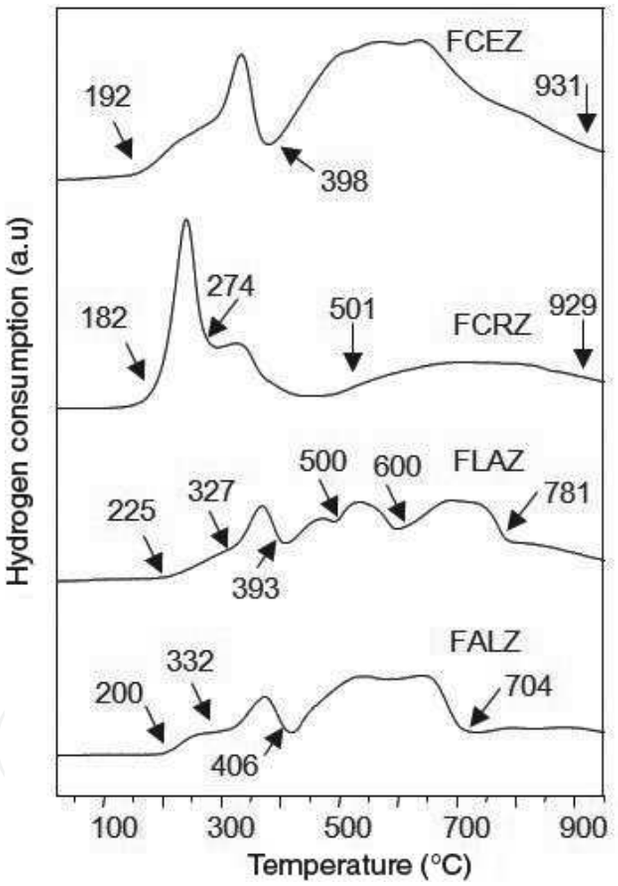

Figure 4. Curves of temperature-programmed reduction for the catalysts. F, iron; CE, cerium; CR, chromium; AL, aluminum; LA, lanthanum; Z, zirconia.

3.6. Activity and selectivity of the catalysts

Figure 5 shows the values of ethylbenzene conversions as a function of temperature during the dehydrogenation with carbon dioxide. It can be noted that the samples were more active

http://dx.doi.org/10.5772/64186

than a commercial catalyst, for all temperature ranges. Also, the catalysts showed different performances, depending on the reaction temperature. At low temperatures, the cerium-based sample led to the highest conversion that, however, decreased with the temperature increase. This can be related to the ability of cerium oxide (detected by X-ray diffraction) for providing lattice oxygen, which activates the carbon dioxide molecule and then increases the reaction rate [32, 33]. The chromium-doped catalyst was the second most active one, leading to conversions of around 46%, which increased with temperature, a fact that can be associated to the high dehydrogenation activity of chromium compounds [16]. The aluminum-doped and lanthanum-doped samples showed similar behaviors, leading to low conversions that increased with temperature.

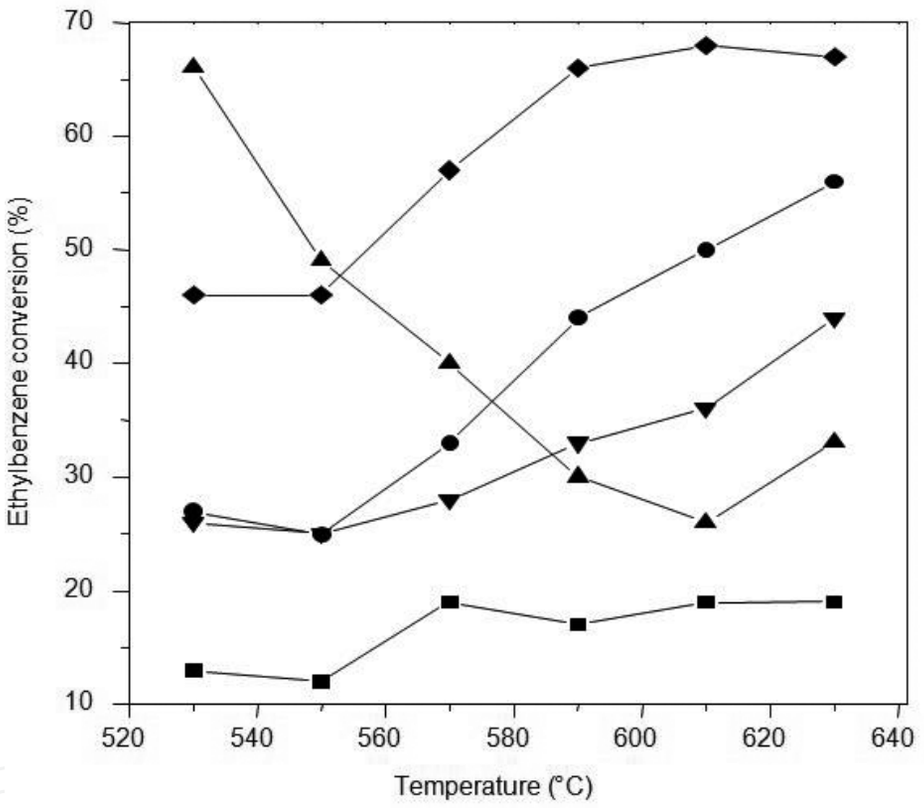

Figure 5. Ethylbenzene conversion over the obtained catalysts and over a commercial catalyst. F, iron; CE, cerium; CR, chromium; AL, aluminum; LA, lanthanum; Z, zirconia.

The selectivity of the catalysts to styrene (**Figure 6**) also changed with the kind of the dopant and with temperature. The aluminum-doped catalyst was the most selective one, but the selectivity decreased as the temperature increased. A similar behavior was noted for the commercial catalyst. On the other hand, the selectivity of cerium-doped sample showed a maximum at around 570°C, while the selectivity of lanthanum-based and chromium-based solids almost did not change with temperature. These findings can be related to the kind of the dopants and their different interactions with the support, as well as to the reaction temperature.

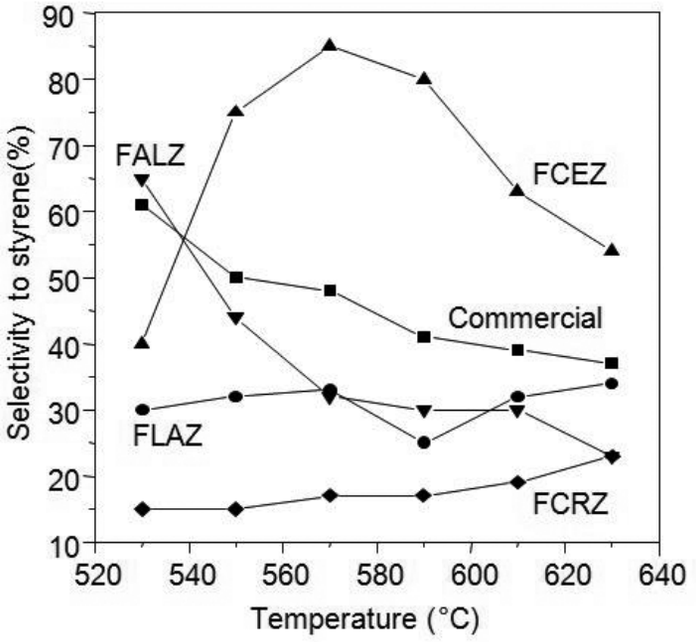

Figure 6. Selectivity to styrene of the obtained catalysts and of a commercial catalyst, during ethylbenzene conversion. F, iron; CE, cerium; CR, chromium; AL, aluminum; LA, lanthanum; Z, zirconia.

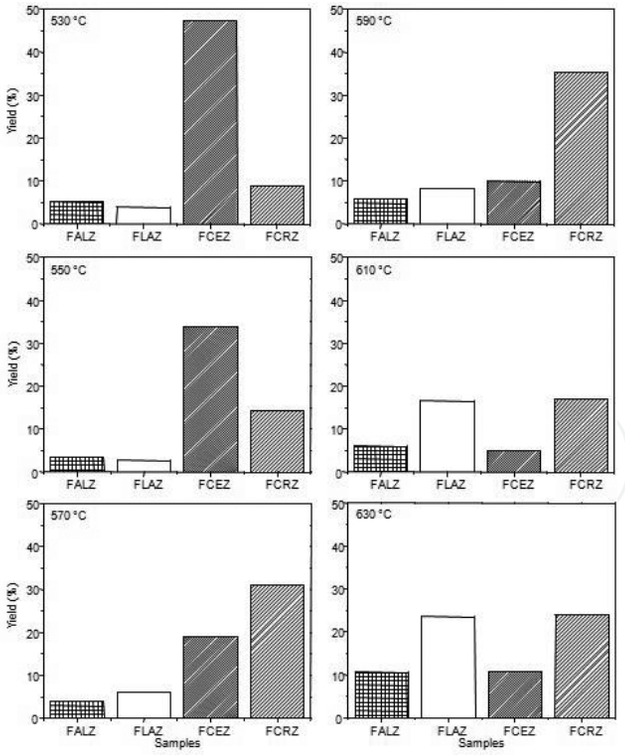

Figure 7. Styrene yields over the obtained catalysts and over a commercial catalyst, during ethylbenzene conversion. F, iron; CE, cerium; CR, chromium; AL, aluminum; LA, lanthanum; Z, zirconia.

http://dx.doi.org/10.5772/64186

Figure 7 shows the yields obtained over the catalysts. One can see that the yield largely depends on the reaction temperature and on the kind of the dopant. The highest value was obtained at 530 and 560°C, over the cerium-doped catalyst. However, the yield decreased with temperature increase, suggesting the catalyst deactivation at high temperatures. While the other catalysts showed low yields for all temperature ranges, the chromium-doped catalyst led to a yield of around 35% at 590°C.

4. Conclusions

Catalysts based on iron oxides (hematite and/or maghemite), supported on zirconium oxide doped with cerium, chromium, aluminum, or lanthanum, show different textural and catalytic properties in ethylbenzene dehydrogenation with carbon dioxide. These findings can be related to the different phases of the supports, such as zirconia (monoclinic or tetragonal), iron oxides (hematite or maghemite), cerium oxide (cubic), lantana (monoclinic or hexagonal), and chromium oxide (rhombohedral), which are also active in the reaction.

The most promising sample was the cerium-doped solid, which led the highest yield (46%) at the lowest temperature. This was assigned to the role of cerium oxide in providing lattice oxygen, which activates carbon dioxide and increases the reaction rate.

The catalysts have proven to provide another alternative to use carbon dioxide, one of the main greenhouse gas and then to contribute to the environment protection.

Acknowledgements

SBL and SMSB acknowledge CAPES and CNPq for their fellowships. The authors thank CNPq and FINEP for the financial support.

Author details

Maria do Carmo Rangel[1,2*], Sirlene B. Lima[1,2], Sarah Maria Santana Borges[1] and Ivoneide Santana Sobral[1]

*Address all correspondence to: mcarmov@ufba.br

1 Grupo de Estudos em Cinética e Catálise, Instituto de Química, Universidade Federal da Bahia, Campus Universitário de Ondina, Salvador, Bahia, Brazil

2 Programa de Pós-Graduação em Engenharia Química, Rua Aristides Novis, Salvador, Bahia, Brazil

References

[1] Abass AO. Valorization of greenhouse carbon dioxide emissions into value-added products by catalytic processes. Journal of CO_2 Utilization. 2013;3-4:74–92. DOI: 10.1016/j.jcou.2013.10.004

[2] Quéré CL, Peters GP, Andres RJ, Andrew RM, Boden T, Ciais P, Friedlingstein P, et al. Global carbon budget. Earth System Science Data Discussion. 2013;6:689–760. DOI: 10.5194/essdd-6-689-2013

[3] IPCC, Climate Change 2013: The Physical Science Basis, Intergovernmental Panelon Climate Change [Internet]. 2013. Available at: https://www.ipcc.ch/report/ar5/wg1/ [Accessed: 2016-02-11].

[4] Honisch B, Ridgwell A, Schmidt DN, Thomas E, Gibbs SJ, Sluijs A, Zeebe R, Kump L, Martindale RC, et al. The geological record of ocean acidification. Science. 2012;335:1058–1063. DOI: 10.1126/science.1208277

[5] Crowley TJ, Berner RA. Enhanced: CO2 and climate change. Science. 2001;292:870–872. DOI: 10.1126/science.1061664

[6] Spigarelli BP, Kawatra SK. Opportunities and challenges in carbon dioxide capture. Journal of CO2 Utilization. 2013;1:69–87. DOI: 10.1016/j.jcou.2013.03.002

[7] Ciferno JP, Fout TE, Jones AP, Murphy JT. Capturing carbon from existing coal fired power plants. Chemical Engineering Progress. 2009;105:33–41. ISSN: 03607275

[8] D'Alessandro DM, Smit B, Long JR. Carbon dioxide capture: Prospects for new materials. Angewandte Chemie International Edition. 2010;49:6058–6082. DOI: 10.1002/anie.201000431

[9] Cuéllar-Franca RM, Azapagic A. Carbon capture, storage and utilisation technologies: A critical analysis and comparison of their life cycle environmental impacts. Journal of CO2 Utilization. 2015;9:82–102, DOI: 10.1016/j.jcou.2014.12.001

[10] Markewitz P, Kuckshinrichs W, Leitner W, Linssen J, Zapp P, Bongartz R, Schreiber A, Müller TE. Worldwide innovations in the development of carbon capture technologies and the utilization of CO_2. Energy and Environmental Science. 2012;5:7281–7305. DOI: 10.1039/C2EE03403D

[11] Vo HT, Imai T, Ho TT, Dang T-L, Hoang SA. Potential application of high pressure carbon dioxide in treated wastewater and water disinfection: Recent overview and further trends. Journal of Environmental Sciences. 2015;36:38–47. DOI: 10.1016/j.jes.2015.04.006

[12] Plasseraud L. Carbon Dioxide as Chemical Feedstock. In: Aresta, M, editor. Chem Sus Chem; 2010. p. 631–632. DOI: 10.1002/cssc.201000097

[13] Boxun H, Curtis G, Steven LS. Thermal, electrochemical, and photochemical conversion of CO_2 to fuels and value-added products. Journal of CO2 Utilization. 2013;1:18–27. DOI: 10.1016/j.jcou.2013.03.004

[14] Aresta M, Dibenedetto A. Product review. The contribution of the utilization option to reducing the CO_2 atmospheric loading: Research needed to overcome existing barriers for a full exploitation of the potential of the CO_2 use. Catalysis Today. 2004;98:455–462. DOI: 10.1016/j.cattod.2004.09.001

[15] Nakagawa K, Okamura M, Ikenaga N, Suzuki T, Kobayashi T. Dehydrogenation of ethane over gallium oxide in the presence of carbon dioxide. Chemical Communications. 1998;9:1025–1026. DOI: 10.1039/A800184G

[16] Wang S, Murata K, Hayakawa T, Hamakawa S, Suzuki K. Dehydrogenation of ethane with carbon dioxide over supported chromium oxide catalysts. Applied Catalysis A. 2000;196:1–8. ISSN: 0926-860X. DOI:10.1016/S0926-860X(99)00450-0

[17] Shimada H, Akazawa T, Ikenaga N, Suzuki T. Dehydrogenation of isobutane to isobutene with iron-loaded activated carbon catalyst. Applied Catalysis A. 1998;168:243–250. ISSN: 0926-860X. DOI:10.1016/S0926-860X(97)00350-5

[18] Mimura N, Takahara I, Saitoa M, Hattorib T, Ohkumac K, Andod M. Dehydrogenation of ethylbenzene over iron oxide-based catalyst in the presence of carbon dioxide. Catalysis Today. 1998;45:61–64. DOI:10.1016/S0920-5861(98)00246-6

[19] Rangel MC, Monteiro AM, Oportus M, Reyes P, Ramos MS, Lima SB. Ethylbenzene dehydrogenation in the presence of carbon dioxide over metal oxides. In: Guoxiang, L, editor. Greenhouse Gases: Capturing, Utilization and Reduction. Publishing Intech; 2012. p. 117–136. ISBN: 978953-51-0192-5

[20] Rangel MC, Monteiro APM, Marchetti SG, Lima SB, Ramos MS. Ethylbenzene dehydrogenation in the presence of carbon dioxide over magnesia-supported iron oxides. Journal of Molecular Catalysis A, Chemical. 2014;387:147–155. DOI:10.1016/j.molcata.2014.03.002

[21] Rangel MC, de Araújo GC, de Lima SM, Assaf JM, Peña MA, Fierro JLG. Catalytic evaluation of perovskite-type oxide $LaNi_{1-x}Ru_xO_3$ in methane dry reforming. Catalysis Today. 2008;133-135:129–135. DOI:10.1016/j.cattod.2007.12.049

[22] Nishiyama T, Aika K. Mechanism of the oxidative coupling of methane using CO_2 as an oxidant over PbO-MgO. Journal of Catalysis. 1990;122:346–351. DOI:10.1016/0021-9517(90)90288-U

[23] Corberán VC. Novel approaches for the improvement of selectivity in the oxidative activation of light alkanes. Catalysis Today. 2005;99:33–41. DOI:10.1016/j.cattod.2004.09.055

[24] Betiha MA, Rabie AM, Elfadly AM, Yehia FZ. Microwave assisted synthesis of a VOx-modified disordered mesoporous silica for ethylbenzene dehydrogenation in pres-

ence of CO_2. Microporous and Mesoporous Materials. 2016;222:44–54. DOI: 10.1016/j.micromeso.2015.10.009

[25] Nederlof C, Kapteijn F, Makkee M. Catalysed ethylbenzene dehydrogenation in CO_2 or N_2-Carbon deposits as the active phase. Applied Catalysis A. 2012;417-418:163–173. DOI:10.1016/j.apcata.2011.12.037

[26] Mamedov EA, Corberan VC. Oxidative dehydrogenation of lower alkanes on vanadium oxide-based catalysts. The present state of the art and outlooks. Applied Catalysis A. 1995;127:1–40. DOI:10.1016/0926-860X(95)00056-9

[27] Sakurai Y, Suzaki T, Nakagawa K, Ikenagaa N-O, Aota H, Suzuki T. Dehydrogenation of ethylbenzene over vanadium oxide-loaded mgo catalyst: Promoting effect of carbon dioxide. Journal of Catalysis. 2002;209:16–24. Doi:10.1006/jcat.2002.3593

[28] Hong D, Vislovskiy VP, Hwang YK, Hung SHJ, Chang J. Dehydrogenation of ethylbenzene with carbon dioxide over MgO-modified Al2O3-supported V-Sb oxide catalysts. Catalysis Today. 2008;131:140–145. DOI:10.1016/j.cattod.2007.10.020

[29] Burri A, Jiang N, Yahyaoui K, Park S-E. Ethylbenzene to styrene over alkali doped TiO2-ZrO_2 with CO_2 as soft oxidant. Applied Catalysis A: General. 2015;495:192–199. DOI: 10.1016/j.apcata.2015.02.003

[30] Zhang S-J, Li W-Y, Li X-H. Effect of preparation methods on the catalytic properties of Fe_2O_3/Al_2O_3-ZrO_2 for ethylbenzene dehydrogenation. Journal of Fuel Chemistry and Technology. 2015;43:437–441. DOI:10.1016/S1872-5813(15)30012-8

[31] Watanabe R, Saito Y, Fukuhara C. Enhancement of ethylbenzene dehydrogenation of perovskite-type $BaZrO_3$ catalyst by a small amount of Fe substitution in the B-site. Journal of Molecular Catalysis A: Chemical. 2015;404-405:57–64. DOI: 10.1016/j.molcata.2015.04.010

[32] Kovacevic M, Agarwal S, Mojet BL, Ommen JGV, Lefferts L. The effects of morphology of cerium oxide catalysts for dehydrogenation of ethylbenzene to styrene. Applied Catalysis A: General. 2015;505:354–364. DOI: 10.1016/j.apcata.2015.07.025

[33] Li X, Feng J, Fan H, Wang Q, Li W. The dehydrogenation of ethylbenzene with CO_2 over $Ce_xZr_{1-x}O_2$ solid solutions. Catalysis Communications. 2015;59:104–107. DOI: 10.1016/j.catcom.2014.10.003

[34] Zarubina V, Talebi H, Nederlof C, Kapteijn F, Makkee M, Cabrera IM. On the stability of conventionaland nano-structured carbon-based catalystsin theoxidative dehydrogenation of ethylbenzeneunder industrially relevant conditions. Carbon. 2014;77:329–340. DOI: 10.1016/j.carbon.2014.05.036

[35] Oliveira SB, Barbosa DP, Monteiro APM, Rabelo D, Rangel MC. Evaluation of copper supported on polymeric spherical activated carbon in the ethylbenzene dehydrogenation. Catalysis Today. 2008;133-135:92–98. ISSN: 09205861. DOI:10.1016/j.cattod.2007.12.040

[36] Delgado JJ, Chen XW, Frank B, Su DS, Schlögl R. Activation processes of highly ordered carbon nanofibers in the oxidative dehydrogenation of ethylbenzene. Catalysis Today. 2012;186:93–98. DOI:10.1016/j.cattod.2011.10.023

[37] Su D, Maksimova NI, Mestl G, Kuznetsov VL, Keller V, Schlögl R, et al. Oxidative dehydrogenation of ethylbenzene to styrene over ultra-dispersed diamond and onion-like carbon. Carbon. 2007;45:2145–2151. DOI: 10.1016/j.carbon.2007.07.005

[38] Ba H, Liu Y, Mu X, Doh W-H, Nhut J-M, Granger P, Pham-Huu C. Macroscopic nanodiamonds/β-SiC composite as metal-free catalysts for steam-free dehydrogenation of ethylbenzene to styrene. Applied Catalysis A: General. 2015;499:217–226. DOI: 10.1016/j.apcata.2015.04.022

[39] Li P, Li T, Zhou JH, Sui ZJ, Dai YC, Yuan WK, et al. Synthesis of carbon nanofiber/graphite-felt composite as a catalyst. Microporous Mesoporous Materials. 2006;95:1–7. DOI:10.1016/j.micromeso.2006.04.014

[40] Qui N, Scholz P, Keller T, Pollok K, Ondruschka B. Ozonated multiwalled carbon nanotubes as highly active and selective catalyst in the oxidative dehydrogenation of ethyl benzene to styrene. Chemical Engineering & Technology. 2013;36:300–306. DOI: 10.1002/ceat.201200354

[41] Vislovskiy VP, Chang J-S, Park M-S, Park S-E. Ethylbenzene into styrene with carbon dioxide over modified vanadia–alumina catalysts. Catalysis Communications. 2002;3:227–231. ISSN: 1566-7367. DOI:10.1016/S1566-7367(02)00105-X

[42] Sun A, Qin Z, Wang J. Reaction coupling of ethylbenzene dehydrogenation with water-gas shift. Applied Catalysis A. 2002;234:179–189. ISSN: 0926-860X. DOI:10.1016/S0926-860X(02)00222-3

[43] Gadalla AM, Livingston TW. Thermal behavior of oxides and hydroxides of iron and nickel. Thermochimica Acta. 1989;145:l–9. DOI:10.1016/0040-6031(89)85121-4

[44] Silva CLS, Marchetti SG, Faro ACJ, Silva TF, Assaf JM, Rangel MC. Effect of gadolinium on the catalytic properties of iron oxides for WGSR. Catalysis Today. 2013;213:127–134. DOI:10.1016/j.cattod.2013.02.025

[45] Pedrosa J, Costa BFO, Portugal A, Durães L. Controlled phase formation of nanocrystalline iron oxides/hydroxides in solution: An insight on the phase transformation mechanisms. Materials Chemistry and Physics. 2015;163:88–98. DOI:10.1016/j.matchemphys.2015.07.018

[46] Martino AD, Iorio M, Prenzler PD, Ryan D, Obied HK, Arienzo M. Adsorption of phenols from olive oil waste waters on layered double hydroxide, hydroxyaluminium–iron-co-precipitate and hydroxyaluminium–iron–montmorillonite complex. Applied Clay Science. 2013;80-81:154–161. DOI:10.1016/j.clay.2013.01.014

[47] Tsipas SA. Effect of dopants on the phase stability of zirconia-based plasma sprayed thermal barrier coatings. Journal of the European Ceramic Society. 2010;30:61–72. DOI: 10.1016/j.jeurceramsoc.2009.08.008

[48] Wiwattanapongpan J, Mekasuwandumrong O, Chaisuk C, Praserthdam P. Effect of dopants on the properties of metal-doped zirconia prepared by the glycothermal method. Ceramics International. 2007;33:1469–1473. DOI: 10.1016/j.ceramint.2006.05.014

[49] Trunschke A, Hoang DL, Radnik J, Lieske H. Influence of lanthana on the nature of surface chromium species in la2o3-modified crox/zro_2 catalysts. Journal of Catalysis. 2000;191:456–466. DOI:10.1006/jcat.1999.2791

[50] Ramos MS, Santos MS, Gomes LP, Albornoz A, Rangel MC. The influence of dopants on the catalytic activity of hematite in the ethylbenzene dehydrogenation. Applied Catalysis A. 2008;341:12–17. DOI:10.1016/j.apcata.2007.12.035